Nat Hazards (2013) 65:315–330
DOI 10.1007/s11069-012-0365-4

ORIGINAL PAPER

Soft computing and GIS for landslide susceptibility assessment in Tawaghat area, Kumaon Himalaya, India

D. Ramakrishnan · T. N. Singh · A. K. Verma · Akshay Gulati · K. C. Tiwari

Received: 20 December 2011 / Accepted: 17 August 2012 / Published online: 9 September 2012

Abstract This paper mainly presents a case study of landslide vulnerability zonation along Tawaghat-Mangti route corridor in Kumaon Himalaya, India. An attempt is made to predict landslide susceptibility using back-propagation neural network (BPNN) and propose a suitable model for that zone, which can be successfully implemented for the prevention of slides. Various landslide affecting parameters such as lithology, slope, aspect, structure, geotechnical properties, land use, landslide inventory, and distance from recorded epicenter are used to model the landslide susceptibility. The database on the above parameters derived from satellite imageries, topographic maps, and field work are integrated in the GIS to generate an information layer. Database of this information layer is used to train, test, and validate the BPNN model. A three-layered BPNN with an input layer, two hidden layers, and one output layer is found to be optimal. The developed model demonstrates a promising result, and the prediction accuracy has been found to be 80 % in the field.

Keywords Kumaon Himalaya · Landslide susceptibility · GIS · BPNN

1 Introduction

The Kumaon Himalayas, lying between the Kali River in the east and Sutlej in the west, include a 320 km stretch of mountainous terrain. The lesser Kumaon Himalaya includes a thrust-bound sector delineated by two tectonic planes—the Main Boundary Fault to the south and the Main Central Thrust to the north. Kumaon Himalaya is located near the central part of the Himalayan orogeny and is, therefore, a critical area for studying the typical characteristics of the Himalayan tectonics, in contrast to the areas in close proximity to NE and NW syntaxes where complications arise due to complex tectonics. Akin to

D. Ramakrishnan · T. N. Singh (✉) · A. K. Verma · A. Gulati
Department of Earth Sciences, Indian Institute of Technology, Mumbai 400076, India
e-mail: tnsingh@iitb.ac.in

K. C. Tiwari
Department of Geology, M.S. University of Baorda, Vadodara 390002, India

other parts of Himalayan orogenic belt, the Kumaon region also possesses prominent topographical features such as escarpment slopes, cliffs, and gorges developed due to complex, physical, geologic, and tectonic processes. Active tectonism and high rate of rainfall coupled with anthropogenic interference have resulted in several catastrophic landslides in this region. The investigated area, Tawaghat-Mangti route corridor is one such worst landslide affected areas in the Kumaon Himalaya and cause serious damages to life and properties annually. Assessment of landslide hazard susceptibility is one of the key tasks in disaster and management in this area.

Artificial neural networks (ANNs) are networks of highly interconnected neural computing elements that have the ability to respond to input stimuli and to learn to adapt to the environment. ANNs include two working phases, the phase of learning and that of recall. During the learning phase, known data sets are commonly used as a training signal in input and output layers. Recall is the proper processing phase for a neural network, and its objective is to retrieve the information. Recall corresponds to the decoding of the stored content, which may have been encoded in network previously. Later, if the network is presented with a pattern similar to a member of the stored set, it may associate the input with the closest stored pattern. The process is called auto-association. Architecture or model of ANNs can be classified on the basis of number of layers and approach that will be undertaken for training. Weights are assigned to the connections between nodes of processing units, and each node has an algorithm for summing the input weights and rule for calculating the output weight. The network is finalized by selecting appropriate transfer functions that allows communication between nodes of respective layers. In this study, interrelationship among different landslide conditioning and triggering variables were modeled using back-propagation neural network (BPNN) and a landslide vulnerability map is produced.

In this study, an integrated approach of remote sensing, geographic information system (GIS), and ANN are used in random to generate spatial database (on landslide conditioning parameters such as slope, lithology, land use, aspect, and anthropogenic interferences), its analysis, and predictive modeling.

2 Literature review

Most of the conventional landslide hazard analyses take into account a reliable and up-to-date landslide inventory that represents the fundamental tool for the identification of the role played by different hill slope instability factors in predisposing and triggering landslides. These approaches are either based on deterministic hazard analysis (Genevois and Tecca 1987; Hammond et al. 1992) or on statistical techniques such as multivariate, discriminate, and probabilistic analysis (Carrara et al. 1991, 1995; Jade and Sarkar 1993; Clerici et al. 2002; Chung et al. 1995; Saha et al. 2005; Lee et al. 2002; Suzen and Doyuran 2004; Ramakrishnan et al. 2005). The final product of such statistical techniques is a function that allows the totaling of a score for each terrain unit, thus expressing the probability of predicting a landslide (Carrara et al. 1995; Ramakrishnan et al. 2005).

After the literature survey of various methods for the prediction of landslide movements, every method is found to be deficient in more than one ways (Sarkar et al. 2008; Singh et al. 2008; Ramakrishanan et al. 2008). On the basis of detailed investigation, a viable approach for the prediction of mass movement is necessary, and an artificial neural network (ANN) comes in handy to fulfill this approach. ANN is gaining significance in

landslide-related modeling by virtue of its capability to handle case-specific, nonlinear relationship among the conditioning and triggering factors. ANNs have been applied to the prediction of rock parameters and landslides in particular, with reference to the determination of the triggering parameters (Aleotti and Chowdhury 1999; Mayoraz et al. 1996; Singh et al. 2004), landslide susceptibility analysis (Lee et al. 2002, 2004; Ferna'ndez-Steeger et al. 2002), and spatial mapping of hazard zones (Ermini et al. 2005). Artificial neural network takes an edge over other conventional methods due to its capability of mapping the nonlinear relations, thus enabling to determine the relationship among complex data pattern (Rumelhart et al. 1986) and to generalize (Widrow et al. 1962). Here, generalization refers to the ability of the neural networks to produce reasonable outputs for inputs not encountered during the training (learning) procedure.

3 The study area

The investigated area (Fig. 1) is located in the northeastern part of the Indian State of Uttarakhand bordering Nepal. The Tawaghat-Jipti route corridor (80°34′53″/29°56′21″–80°44′16″/30°00′00″) runs all along the Kali river valley for about 30 km distance. Physiographically, this part of Himalayan province rises to an elevation of 1,500–2,500 m and exhibits an active tectonics-related topography. Geologically, the investigated area comprises rock of lesser Himalayan meta-sedimentaries (phyllite, schists, micaceous quartzites, and amphibolites) and crystalline rocks like granitic gneiss. The investigated area receives an average annual rainfall of 2,200 mm mostly confined to monsoonal months (July–September). Sudden cloud burst with a very heavy rainfall (150–200 mm/day) is a recurrent phenomenon in this area. This area experiences frequent landslides and alarming rate of erosion.

4 Methodology and thematic database generation

In this study, a variety of data related to the study of landslides such as satellite images, digital elevation model, geological map, and rainfall are used. The spatial data on rock types and structure are obtained from the published maps of Geological Survey of India. Geotechnical parameters such as RQD for each litho units are estimated from the field. Calibrated digital elevation model (DEM) derived from shuttle radar topographic mission (SRTM) is used to derive the slope map. Slope map of the study area is derived from the calibrated SRTM-DEM using ERDAS imagine inbuilt inverse distance weighted (IDW) interpolation technique. Land use maps are prepared using Indian remote sensing satellite (IRS-LISS-IV) data. Integration of vector coverage and collateral data is carried out using ARC/Info GIS software. The course of investigations adopted is given in Fig. 2. The attribute table of the output layer with unique identity for each polygon and information on conditioning and triggering parameters is used as an input for ANN analyses. Brief description about the derived thematic database is given below.

4.1 Lithology and geotechnical characteristics

Lithology of the study area comprises 11 major rock types namely quartzite, biotite gneiss, chlorite schist, amphibolite, micaceous quartzite, carbonaceous phyllite, calc-silicate, talc chlorite schist, phyllite, graphite schist, along with unconsolidated rocks such as talus/scree

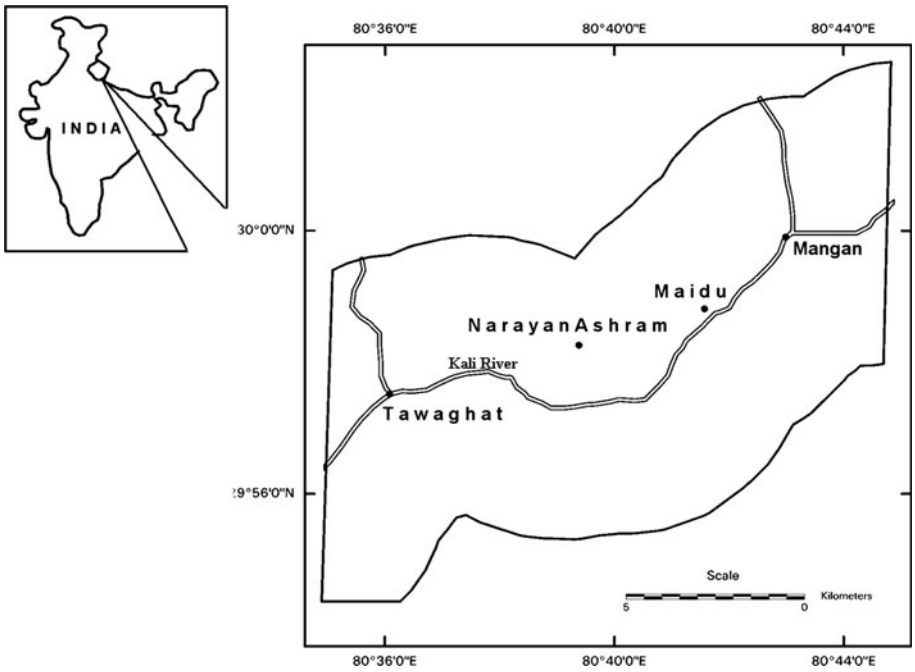

Fig. 1 Location map of the study area

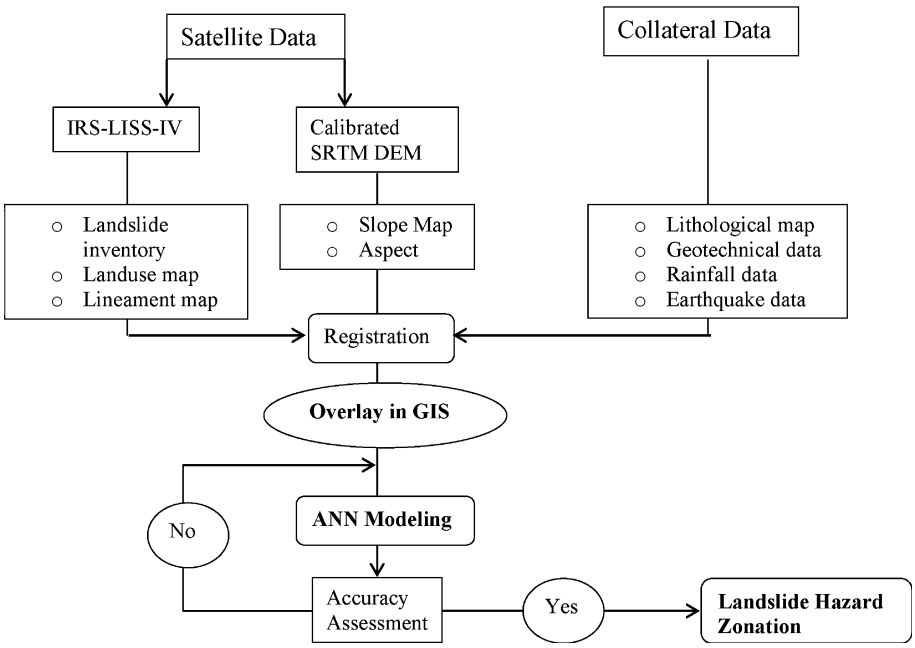

Fig. 2 Flow chart depicting the adopted methodology

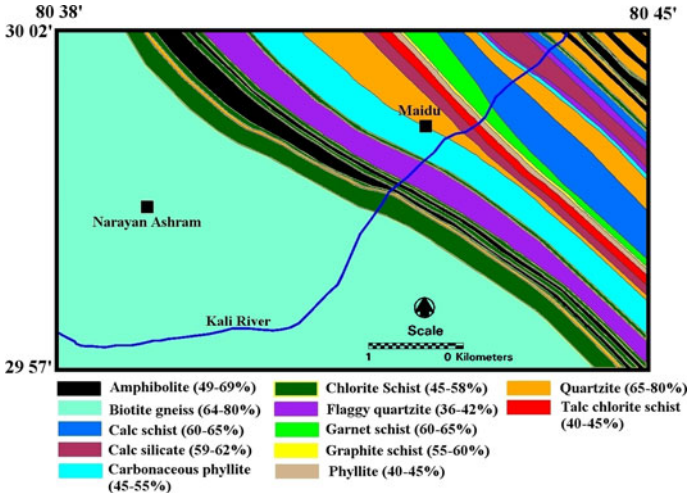

Fig. 3 Lithological map of the study area. Values in parenthesis indicate the RQD

deposits (Fig. 3). The meta-sedimentary rocks are characterized by 4–5 sets of discontinuity planes. The geotechnical quality of rock mass expressed through the rock quality designation (RQD) is derived for each of the above said rock types and added as an attribute to the lithology vector layer. The rock quality designation (RQD) value of each litho unit is estimated using the following empirical relationship (Palmstrom 1982)

$$\mathrm{RQD} = 115 - 3.3J_V$$

where J_v—total number of joints per m^3. RQD of 100 is considered when J_v exceeds 4.5. The estimated RQD values vary from 64 to 80 %.

4.2 Landslide inventory and land use

Information on landslide inventory and land use is very crucial for slope stability studies. Since reactivation of existing landslides is one of the commonest mode of slope failures, inventory of stabilized and active landslides is generated from satellite imaginary (IRS-LISS-IV) for the periods May and October 2002. Information on land use and pattern of their spatial distribution is derived by classifying the above satellite data by supervised classification technique using the Bayesian maximum likelihood classifier (MLC). MLC, a parametric decision rule, is a well-developed method from statistical decision theory that has been applied to the problem of classifying image data (Settle and Briggs 1987). Information collected from the state forest department, survey of India (SOI) topographic maps and field studies on the watershed area used to identify the signatures representing various land use classes. They are then evaluated to make sure that, there is suitable discrimination of individual classes. After obtaining a suitable grouping for satisfactory discrimination between the classes during signature evaluation, the final classification is carried out. The classification accuracy evaluated by confusion or error matrix showed 92 and 95 % accuracy for the producer and the user estimates, respectively. In all, eight major land use classes, namely open forest, dense forest, scrub land, plantation, active/stabilized landslides, barren/rocky, fallow, river bed, have been considered (Fig. 4).

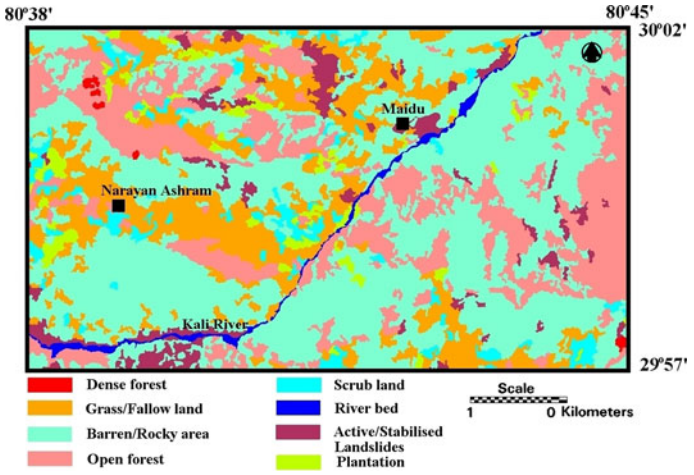

Fig. 4 Land use/land cover map of the area indicating the spatial distribution of active and stabilized landslides

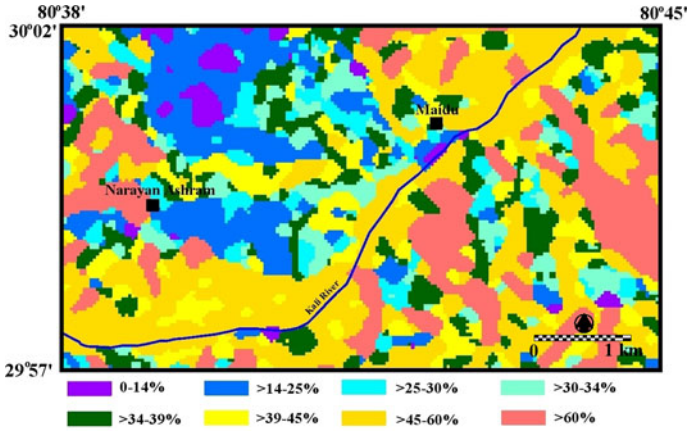

Fig. 5 Slope map of the area

4.3 Slope and aspect

Since, slope is a vital conditioning parameters for slope instability, an accurate slope map is necessary in identifying the landslide vulnerable areas. In this study, a slope map is prepared using the calibrated SRTM-DEM. The finished and filled SRTM-DEM is calibrated with information on latitude, longitude, and altitude collected in the field with differential global position system (DGPS). In all, data from 72 ground control points (GCP) are used to fit a second-order polynomial equation and calibrate the DEM. The slope map is classified into eight categories such as <14, 14–25, >25–30, >30–34, >34–39, >39–45, >45–60, and >60 % (Fig. 5). These eight categories of slope were made based on the Jenks natural breaks optimization technique (Jenks 1967). Such classification was

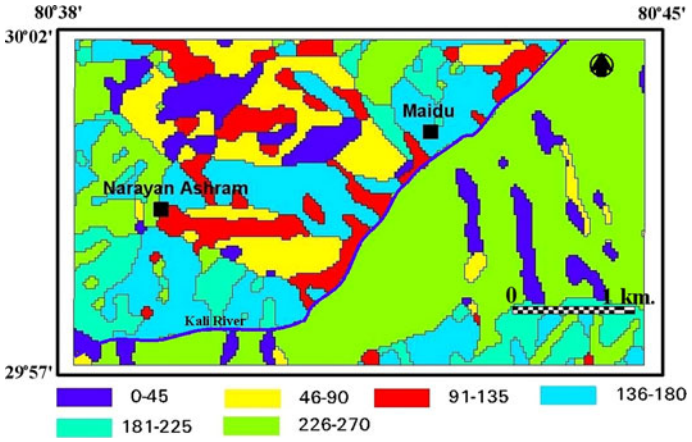

Fig. 6 Prevailing aspect classes of the area (values are in degrees)

observed to be efficient in portraying the terrain-specific information content relating the slope and landslide vulnerability (Ramakrishnan et al. 2005).

The direction of slope face (aspect) plays an important role in controlling different types (plane, wedge, toppling, and soil) of slope failures. Formation of wedge and daylight surface is a function of interrelation among strike, dip of the discontinuities, and slope face. In this study, the aspect map is generated (Fig. 6) from the DEM and classified into eight classes like 0–45; 45–90, 90–135, 135–180, 180–225, 225–270, 270–315, and 315–360 degrees.

4.4 Geological structure/lineament

Fractures, rock cleavages, and fault/thrust play a vital role in affecting the rock mass quality and pore pressure built-up. The above linear features (lineaments) can be measured and mapped from the toposheets and satellite images. In this study, lineament map is prepared from the satellite data following the edge enhancement techniques and field checks (Fig. 7). In all, three predominant lineament trends bearing azimuth direction 10°, 48°, and 90° trends are observed. These lineaments are classified as major (thrusts and faults running over 1 km.) and minor (fractures running lesser than 1 km) based on their length of continuity. After critical field evaluation, the major and minor lineaments are buffered to (100, 50, and 5 m distances, respectively, for thrust, fault, and fracture) represent their spatial influence.

4.5 Anthropogenic interference

In the study area, cut slopes for the road is the major anthropogenic interference. Building loads alter the earth pressure in the slopes, and frequent vibrating loads from traffic affect the slope stability. It is found that the embedded depth of some building foundations were higher than that of retaining walls, which meant the building foundations failed to lie in stable horizons. Deformation of the buildings and slopes should be monitored; control measures such as cutting off the beams of reinforced concrete and use of anti-slide piles should be taken to control lateral deformation of the slopes or the retaining walls. Cut

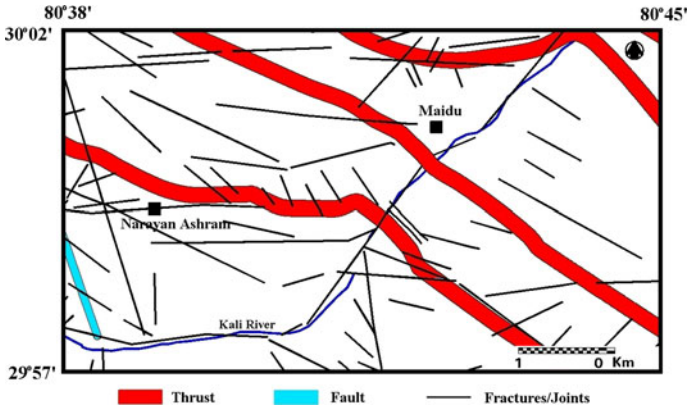

Fig. 7 Field validated lineament map indicating the major structural features

slopes and associate roads are classified into two categories such as treated (where the slopes are provided with drain holes, meshes, and the roads are asphalted) and untreated (where no treatments are done).

5 Results and discussions

Prior to selecting any of the conventional method for assessing the landslide susceptibility, it is important to determine the weight value representing different factors according to their importance for landslide occurrence. Conventionally, the weights are assigned on the basis of the experience of the experts about the subject and the area (Lee et al. 2004). This weighting system was highly subjective and might therefore contain some implicit biases toward the assumptions made (Lee et al. 2004). In this study, an attempt is made to derive the weights for individual conditioning and triggering parameters using BPNN so as to reduce the biases and associated errors.

5.1 Artificial neural network weighting procedure

Multilayer feed forward model network was selected because of its efficiency and also found to be an appropriate one in this case. It generally consists of three layers, that is, input, hidden, and output layer. Number of neurons in the input layer depends on the number of input data sources. Input in the form of neurons comprises the first layer and each neuron is connected to the neuron of the successive layer, where each connection is carrying the initial set weights. Features extracted from the thematic layers are used as input in the input layer, number of hidden layers and number of neurons in the hidden layers are determined by the hit and trial process.

One of the basic element of the any ANNs architecture is the squashing function or signal function. The role of the signal function is to squash (limit) the output signal of the neuron to a certain (finite) range. Squashing function maps a (possibly infinite) domain (the input) to a prespecified range (the output). A great number of mathematical functions should be suitable for the role of the activation function of a neuron. Any nonlinear function can be used as a squashing function, but a tan-sigmoid function which constrains

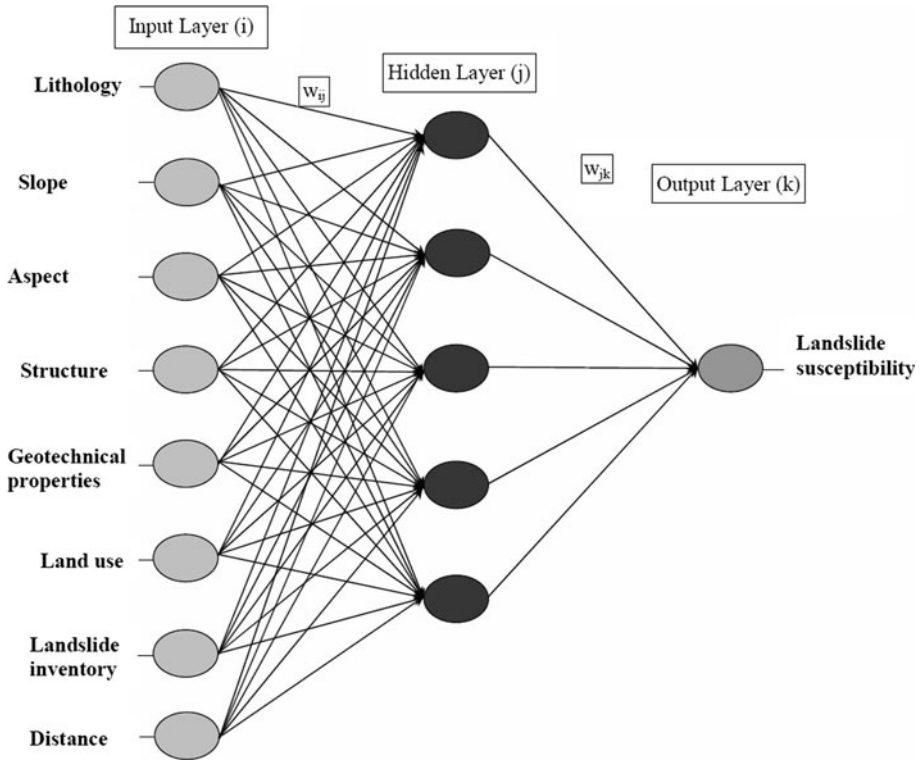

Fig. 8 Back-propagation neural network

the output of network between 0 and 1 is widely in use (Gill et al. 1981; Sinha et al. 2009). A schematic diagram of the most appropriate model is given in Fig. 8.

5.1.1 Training

Network weights are adjusted during the training sessions and the application of the learning rule. Learning is realized through updation at synaptic, neural and network levels, as it take place in the entire network.

One of the widely used paradigms of learning algorithm in neural network is the back-propagation learning algorithm (BPLA). The BPLA is applied on multilayer feed forward networks, also known as multilayer perceptrons (MLP). It is based on an error correction learning rule, that is, on the minimization of the mean squared error that is a measure of the difference between the actual and the desired output, and is the most commonly used generalization of the "delta rule." There are number of algorithms which are based on back-propagation learning (Ripley 1996; Haykin 1999; Zhou 1999; Gomez and Kavzoglu 2005; Zurada 2006). Most frequently used back-propagation algorithms are gradient descent and gradient descent with momentum.

The algorithm is based on the back-propagation of the errors (the differences between the actual and the desired output). The simulation of algorithm involves two phases, the forward phase that occurs when the inputs (external stimuli) are presented to the neurons of the input layer and propagated forward to compute the output, and the backward phase

Table 1 Parameters for network

Parameter	Values
Learning parameters	8
Momentum parameters:	0.7
Networks training function	Trainoss
Activation (transfer) function for all layers	Tansig

when the algorithm performs modifications in the backward direction. With respect to the convergence rate, the back-propagation algorithm is relatively slow and often too slow for the solution of practical problems. This is mainly due to the stochastic nature of the algorithm that provides an instantaneous estimation of the gradient of the error surface in weight space. When the error surface is fairly flat along a weight dimension, the derivative of the error surface with respect to that weight is small in magnitude; therefore, the synaptic adjustment applied to the weight is small, and thus many iterations (epochs) of the algorithms may be required to produce a significant reduction in the error performance of the network. However, faster algorithms use standard numerical optimizers such as conjugate gradient (Powell 1977), quasi–Newton, and Levenberg–Marquardt approach (Battiti 1992). In this study, quasi-Newton algorithm (implemented as TRAINOSS in MATLAB software) has been use for training the network. The neural network processing has been implemented in Neural Network tool box of MATLAB software. The characteristic functioning aspects of the network are given in Table 1.

Trainoss is of the quasi-Newton algorithm, adapting the one-step secant method to calculate the new search direction without computing a matrix inverse. It works on a principle similar to momentum to reduce oscillation of weight changes.

Tan-sigmoid transfer function maps all inputs to the range of -1 to 1 as shown in Fig. 9.

The training (back-propagation of error) is repeated iteratively until error is minimized to an acceptable value and validation of model is completed. The presentation of the entire training data set during the training process is known as an epoch. When the learning algorithm is applied on an epoch-by-epoch basis, it means back-propagation algorithm is applied in sequential mode or pattern-by-pattern mode. Performance of the network is illustrated (Fig. 10), which plots the plot between time required to converge vs mean square error convergence goal.

The weights obtained at the validation stage of the model can be used for forecasting purpose. The performance of network depends upon the accuracy of the validation of data set. Thus, after data are trained and validated to an acceptable accuracy, the model is used to determine the output of the unknown data set.

In the present study, a multilayer feed forward network with one input layer and two hidden layers and one output layer has been considered. The input layer contains nine neurons, each representing a factor contributing in the occurrence of landslide. Output layer consists of one neuron representing one of the two vulnerability classes (i.e., landslide vulnerable areas and non-vulnerable areas).

The most appropriate neural network architecture based on the accuracy of results was arrived by training and testing different hidden layers and associated neurons. After testing various network combinations, the network with 9-5-7-1 architecture with learning rate of 0.1 and momentum of 0.01 (Table 2) is found to be giving the best results.

The complete data set of the study area is then processed in the identified model to delineate landslide vulnerable areas. For this purpose, the database of the output vector

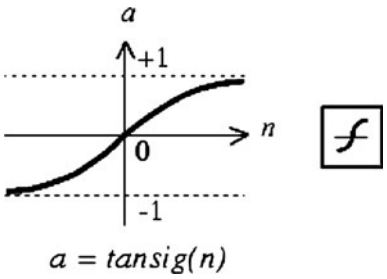

Fig. 9 Tan-sigmoid transfer function

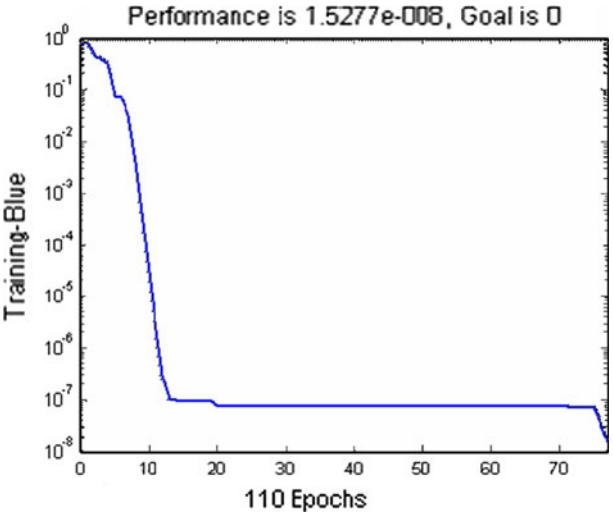

Fig. 10 Epochs versus mean square error for convergence goal of 0

Table 2 Training and testing data accuracies for a 9-5-7-1 architecture with 800 epochs and 2,045 patterns (bold indicates the best acceptable architecture in this study)

Learning rate (η)	Momentum (α)	Absolute error
0.2	0.10	3.98
0.4	0.09	3.60
0.1	0.05	3.45
0.5	0.08	3.33
0.7	**0.01**	**2.84**

layer of overlay analysis is used. Out of 8,060 polygons representing the entire study area, information pertaining to conditioning and triggering parameters of 2,045 polygons is used to establish the relationship (training) between landslide occurrence and influence factors. Rest of 6,015 polygons is used to evaluate the accuracy of prediction (testing) by comparing ANN-derived vulnerability with actual field data on landslide occurrence. In all, 63 events were identified in the entire area. Point coverage of landslide occurrence was overlaid on the ANN-derived results (Fig. 11) and compared for accuracy. Out of 63 occurrences (58 old and 5 new), it is observed that 61 events fall within the high (47 events) and moderate (14 events) vulnerable classes. It is also evident from the recent

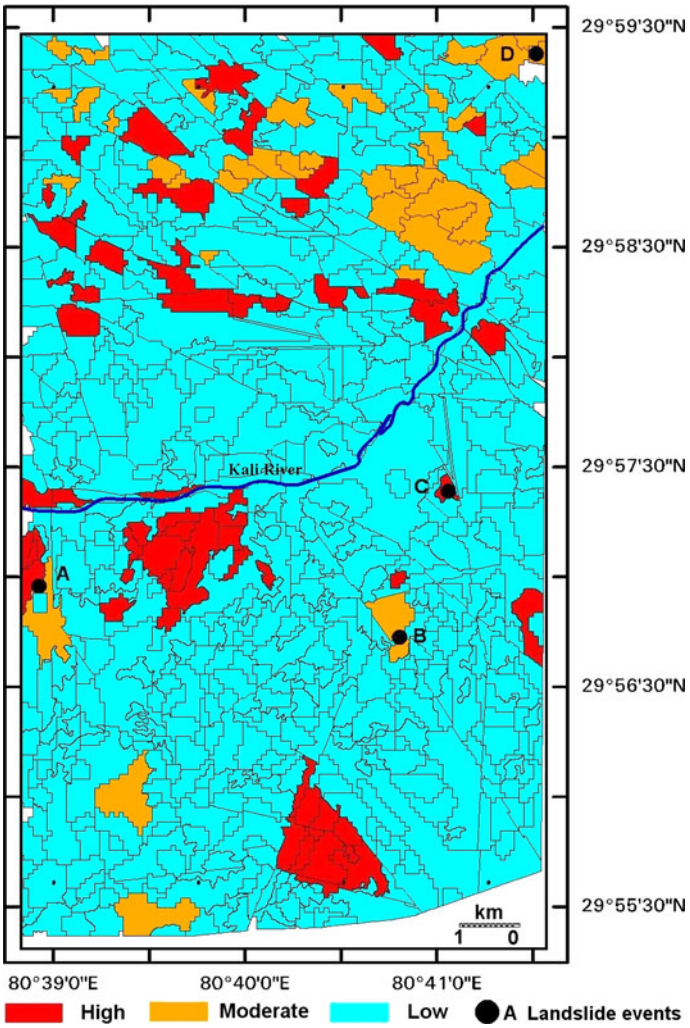

Fig. 11 Landslide hazard vulnerability map

(2010) satellite data (IRS-LISS-IV) that the area has witnessed five new landslides (Table 4) of different dimensions and magnitude. It is interesting to note that 80 % of the new slides occurred in the high vulnerability class.

Details of the optimum weights derived among the input-hidden layer 1–hidden layer 2–output layer are presented in Table 3a, b, c.

The output derived from the network was related to the vector coverage for further spatial analyses and visualization (Fig. 11). Blue lines in the figure show the direction of flowing Kali River. On the basis of histogram distribution, the vulnerability prediction is classified into three classes such as low vulnerability, moderate vulnerability, and high vulnerability for probability ranges 0–0.57, 0.57–0.85, and >0.85, respectively (Table 4).

Table 3 Weight distribution characteristics of the best performing network used in this study

(a) Weights distribution between input (I) and first hidden (HA) layer

Input (I)	HA_1	HA_2	HA_3	HA_4	HA_5
Aspect	−0.8384	0.1292	−0.6218	1.0871	0.4693
Lithology	0.4668	2.5274	0.9371	0.8032	−0.4211
RQD	−0.0299	−0.8582	0.2030	−0.5102	−0.4859
Class	0.4094	−0.1201	0.2559	−0.2501	0.3562
Road type	0.7924	0.9211	−1.1714	1.0019	3.2696
Lithology	−0.6497	0.0736	−0.4444	−0.4868	0.1207
Slope	0.0494	0.0164	0.2131	0.1147	−0.0235
Lineament	0.1377	0.1377	−0.9604	−1.1481	−0.1633
Landslide inventory	−0.8857	−0.8857	0.1228	−0.3271	−0.2621

(b) Weight distribution between first hidden (HA) layer and second hidden layer (HB)

	HA_1	HA_2	HA_3	HA_4	HA_5
HB_1	0.3308	−0.5768	−0.4971	−1.4552	−0.9914
HB_2	0.4123	1.0764	−1.2543	0.1010	1.7734
HB_3	−1.5293	1.4267	−0.3068	1.1991	2.2236
HB_4	−1.3424	0.3373	0.8981	0.7919	−1.4872
HB_5	−0.9338	−1.2779	0.7093	−0.7129	−0.8292
HB_6	0.0003	−1.1531	0.4502	−1.3133	−2.1357
HB_7	−1.2777	−0.1621	0.1593	1.0532	−1.2139

(c) Weight distribution between second hidden layer (HB) and output (O) layer

	Weights
$HB\text{-}Output_1$	0.2645
$HB\text{-}Output_2$	1.6663
$HB\text{-}Output_3$	2.9171
$HB\text{-}Output_4$	−0.8433
$HB\text{-}Output_5$	−0.1401
$HB\text{-}Output_6$	−2.1400
$HB\text{-}Output_7$	0.3901

Table 4 Landslide events vis-à-vis hazard zonation

Location	Latitude and longitude	Area of slide (m^2)	Classified hazard zone
A	80 37 54 N 29 58 39 E	250	Moderate
B	80 39 33 N 29 57 22 E	640	High
C	80 38 55 N 29 56 57 E	450	High
D	29 57 03 N 80 40 55 E	980	High
E	80 41 28 N 29 56 54 E	260	High

6 Conclusions

The Tawaghat-Mangti route corridor of Kumaun Himalayas is one of the worst affected areas due to frequent landslides. This causes serious threat to human lives, properties, and disturbs the supply routes. The interplay between conditioning parameters (lithology, slope, aspect, land use, fracture) and triggering parameters (rainfall, seismicity, and anthropogenic interference) plays a pivotal role in the stability of slopes of this region. It is often difficult to estimate the significance of one parameter over the other in evaluating its criticality in making a slope unstable. Conventional statistical- and heuristic-based approaches try to relate a landslide event to individual contributory parameters through relative weights and ranks. Probability prediction based on such expert-based weights and rank assignments is often subjective and prone to errors (Gupta et al. 2008). From this point, artificial neural network is more generic and fairly considerably accurate in establishing the interrelationship among the variables and associated weight in predictive modeling (Kanungo et al. 2006; Chung and Chao 2006). In this study, BPNN-based weight retrieval was carried out between the failed slopes and different spatial parameters associated with it. Final network architecture with an input layer, two hidden layers (with five and seven neurons, respectively), and an output neuron was arrived after testing number of networks on hit and trial process. Similarly, numbers of trial runs were also performed at different learning rates and momentum to optimize the performance of network. From these trails, learning rate of 0.7 was found to be stable and optimum. When results of the predicted data are compared with the field data, more then 97.16 % results are found to be accurate with an absolute error of 2.84 %, indicating a highly satisfactory prediction model. It is also evident that the accuracy of prediction by ANN is better than the information value-based approaches for the same area (Tiwari et al. 2006).

In this study, the primary and derived data pertaining to different conditioning and triggering parameters were derived from satellite images, field investigations, published maps, and topographic sheets. Spatial and non-spatial data integration and generation of input database for ANN were carried out using the overlay concepts of GIS. The derived database comprises 8,060 individual data sets with information on parameter attributes and presence or absence of a landslide. Out of the total 8,060 data sets, 2,045 were used for training and the rest for testing and validate the network. The output of the ANN predictive model is classified into three probability categories such as 0–0.57, 0.57–0.85, and > 0.85 corresponding to hazard classes low, medium, and high, respectively, on the basis of histogram distribution. Validation of the hazard zones was carried out by analyzing the landslides for a subsequent period. The overall accuracy of the proposed model is 80 %, which indicates the efficacy of methodology adopted and recommended in the present study.

References

Aleotti P, Chowdhury R (1999) Landslide hazard assessment: summary review and new perspectives. Bull Eng Geol Environ 58:21–44

Battiti R (1992) First and second order methods for learning: between steepest descent and Newton's method. Neural Comput 4(2):141–166

Carrara A, Cardinali M, Detti R, Guzzetti F, Pasqui V, Reichenbach P (1991) GIS techniques and statistical models in evaluating landslide hazard. Earth Surf Proc Land 16:427–445

Carrara A, Cardinali M, Guzzetti F, Reichenbach P (1995) GIS technology in mapping landslide hazard. In: Carrara A, Guzzetti F (eds) Geographical information systems in assessing natural hazards. Kluwer, The Netherlands, pp 135–175

Chung CT, Chao RJ (2006) Application of back-propagation networks in debris flow prediction. Eng Geol 85:270–280
Chung CHF, Fabbri AG, Van Western CJ (1995) Multivariate regression analysis for landslide hazard zonation. In: Carrara A, Guzzetti F (eds) Geographical information system in assessing natural hazards. Kluwer, The Netherlands, pp 107–142
Clerici A, Perego S, Tellini C, Vescovi P (2002) A procedure for landslide susceptibility zonation by the conditional analysis method. Geomorphology 48:349–364
Ermini L, Catani F, Casagli N (2005) Artificial neural networks applied to landslide susceptibility assessment. Geomorphology 66:327–343
Ferna'ndez-Steeger TM, Rohn J, Czurda K (2002) Identification of landslide areas with neural nets for hazard analysis. In: Stemnerk J, Wagner P (eds) Landslides. Balkema, The Netherlands, pp 163–168
Genevois R, Tecca PR (1987) Probabilistic analysis of slopes stability: an application for hazard studies in the middle valley of the Tammaro River (southern Italy). Mem Soc Geol Ital 37:157–170 (in Italian)
Gill PE, Murray W, Wright MH (1981) Practical optimization. Academic Press, New York, pp 1–420
Gomez H, Kavzoglu T (2005) Assessment of shallow landslide susceptibility using artificial neural networks in Jabonosa River Basin, Venezuela. Eng Geol 78(1–2):11–27
Gupta RP, Kunango DP, Arora MK, Sarkar S (2008) Approaches for comparative evaluation of raster GIS-based landslide susceptibility zonation maps. Int J Appl Earth Obs Geoinf 10:330–341
Hammond C, Hall D, Miller S, Swetik P (1992) Level I stability analysis (LISA) documentation for version 2.0, General Technical Report INT-285, USDA Forest Service Intermountain Research Station
Haykin S (1999) Neural networks: a comprehensive foundation, 2nd edn. Prentice Hall, New Jersey, p 842
Jade S, Sarkar S (1993) Statistical models for slope instability classification. Eng Geol 36:91–98
Jenks GF (1967) The data model concept in statistical mapping. Int Year Book Cartogr 7:186–190
Kanungo DP, Arora MK, Sarkar S, Gupta RP (2006) A comparative study of conventional, ANN black box, fuzzy and combined neural and fuzzy weighting procedures for landslide susceptibility zonation in Darjeeling Himalayas. Eng Geol 85:3247–3366
Lee S, Choi J, Min K (2002) Landslide susceptibility analysis and verification using the bayesian probability model. Environ Geol 43:120–131
Lee S, Ryu JH, Won JS, Park HJ (2004) Determination and application of the weights for landslide susceptibility mapping using an artificial neural network. Eng Geol 71:289–302
Mayoraz F, Cornu T, Vuillet L (1996) Using neural networks to predict slope movements. In: Proceedings of VII international symposium on landslides. Trondheim, Balkema, Rotterdam, p 295–300
Palmstrom A (1982) The volumetric joint count—a useful and simple measure of the degree of rock mass jointing. In: IAEG Congress, New Delhi, p 221–228
Powell MJD (1977) Restart procedures for the conjugate gradient method. Math Program 12:241–254
Ramakrishanan D, Singh TN, Purwar N, Badre KS, Gulati A, Gupta S (2008) Artificial neural network and liquefaction susceptibility assessment: a case study using the 2001 Bhuj Earthquake data, Gujarat, India. Comput Geosci 12:491–501
Ramakrishnan D, Ghosh MK, Vinuchandran R, Jeyaram A (2005) Probabilistic techniques, GIS and remote sensing in landslide hazard mitigation: a case study from Sikkim Himalayas, India. Geocarto Int 20(4):1–6
Ripley B (1996) Pattern recognition and neural networks. Cambridge University Press, Cambridge, p 416
Rumelhart DE, Hinton GE, Williams RJ (1986) Learning internal representation by error propagation in parallel distributed processing. Massachusetts Institute of Technology Press, Cambridge
Saha AK, Gupta RP, Sarkar I, Arora MK, Csaplovics E (2005) An approach for GIS-based statistical landslide susceptibility zonation—with a case study in the Himalayas. Landslides 2:61–69
Sarkar K, Gulati A, Singh TN (2008) Landslide susceptibility analysis using artificial neural networks and GIS in Luhri area, Himachal Pradesh. J Indian Landslides 1(1):11–20
Settle JJ, Briggs SS (1987) Fast maximum likelihood classification of remotely sensed imagery. Int J Remote Sens 8(5):723–734
Singh TN, Kanchan R, Saigal K, Verma AK (2004) Prediction of P-wave velocity and anisotropic properties of rock using artificial neural networks technique. J Sci Ind Res 63(1):32–38
Singh TN, Gulati A, Dontha L, Bhardwaj V (2008) Evaluating cut slope failure by numerical analysis—a case study. Nat Hazards 47:263–279
Sinha S, Singh TN, Singh V, Verma AK (2009) Epoch determination for neural network by self organised map. Comput Geosci 14(1):199–206
Suzen ML, Doyuran V (2004) A comparison of the GIS based landslide susceptibility assessment methods: multivariate versus bivariate. Environ Geol 45:665–679

Tiwari KC, Ganapathi S, Mehta A, Sharma S, Ramakrishnan D (2006) Landslide hazard zonation of Tawaghat—Jipti Route Corridor,Pithoragarh, Uttaranchal State: Using GIS and probabilistic technique approach. Proceedings of SPIE (Kogan F. Ed.) 6412:1–12

Widrow B, Jovitz MC, Jacobi GT, Goldstein G (1962) Generalization and information storage in networks of adaline'neurons'. In: Self organizing systems. Spartan Books, Washington DC, pp 435–461

Zhou W (1999) Verification of the nonparametric characteristics of back propagation neural networks for image classification. IEEE Trans Geosci Remote Sens 37:771–779

Zurada KJ (2006) Introduction to artificial neural systems. 10th edn. Jaico Publishing House, Mumbai, p 120